Author's post-print version of "O'Reilly, C., & Nielsen, T. (2013). Assessing EEG sleep spindle propagation. Part 2: Experimental characterization. J Neurosci Methods. doi: 10.1016/j.jneumeth.2013.08.014" (http://www.sciencedirect.com/science/article/pii/S0165027013002859)

Title

Assessing EEG sleep spindle propagation. Part 2: Experimental characterization

Authors

Christian O'Reilly, Ph.D & Tore Nielsen, Ph.D.
[christian.oreilly, tore.nielsen]@umontreal.ca

Dream and Nightmare Laboratory
Center for Advanced Research in Sleep Medicine
Hôpital du Sacré-Coeur de Montréal
5400 boulevard Gouin Ouest
Montréal, Québec
H4J 1C5, Canada

Keywords

electroencephalography; sleep spindle; frequency; duration; amplitude; time delay; propagation

Abstract

Background: This communication is the second of a two-part series that describes and tests a new methodology for assessing the propagation of EEG sleep spindles. Whereas the first part describes the methodology in detail, this part proposes a thorough evaluation of the approach by applying it to a sample of laboratory sleep recordings.

New Method: The tested methodology is based on the alignment of time-frequency representations of spindle activity across recording channels and is used for assessing sleep spindle propagation over the human scalp using noninvasive EEG.

Results: Spindle propagation displays features that suggest wave displacements of global synaptic potential fields. Propagation patterns that are coherent (as opposed to random), laterally symmetrical, and highly repeatable within and between subjects were observed. Propagation was slower from posterior to anterior and from central to lateral brain regions than in the opposite directions. Propagation speeds varied between 2.3 and 7.0 m/s were obtained. A distinct grouping of propagation properties was noted for a small cluster of frontal electrodes. No propagation between distantly separated scalp locations was observed. The values of spindle characteristics such as average frequency, RMS amplitude, frequency slope, and duration, depend largely on propagation direction but are only mildly correlated with propagation delay.

Comparison with Existing Method(s): Results obtained are in line with many results published in the literature and offer new measures for describing sleep spindle behavior.

Conclusions: Propagation properties provide new information about sleep spindle behaviors and thus allow more precise automated assessments of spindle-related functions.

1. Introduction

1.1. General context

Sleep spindles are transient electrical events — 0.5 to 3.0-second phasic bursts with an oscillatory activity in the 11 to 16 Hz range — that can be observed using different recording modalities such as electroencephalography (EEG), magnetoencephalography (MEG), and implanted electrodes. They are typically assessed in polysomnographic sleep studies using the EEG; MEG is less widely used because of practical issues of cost, sleep comfort, etc. while implanted electrodes are too invasive to be used in subjects other than animals or epileptic patients. There has been a steady increase in descriptive studies of sleep spindle properties (e.g.,Andrillon et al., 2011; Molle et al., 2011; Peter-Derex et al., 2012) because of accumulating evidence that they are reliably associated with cognitive faculties (Fogel and Smith, 2011), normal aging processes (Crowley et al., 2002), and various disease states (De Gennaro and Ferrara, 2003; Ferrarelli et al., 2010). There has also been substantial work accomplished in the automation of algorithms to detect, count, and describe sleep spindles although the variety of proposed approaches indicates that no consensus on a standard procedure has yet emerged (e.g., Acır and Güzeliş, 2004; Babadi et al., 2012; Causa et al., 2010; Duman et al., 2009; Huupponen et al., 2007; Schimicek et al., 1994; Schonwald et al., 2006; Sinha, 2008; Ventouras et al., 2005; Wendt et al., 2012). These automation efforts aim at saving hours of labor, avoiding the subjective biases of expert scorers, and facilitating discovery. Accordingly, the first part of this two-part series presents a novel computerized methodology to extract information associated with the propagation of EEG sleep spindles across the scalp (O'Reilly and Nielsen, 2013a). The present work describes the application of this method to laboratory sleep recordings and further addresses some important questions raised by the approach. But before presenting our specific research goals, a short presentation of the concept of brain waves as

developed in (Nunez, 1974; Nunez and Srinivasan, 2006b) is provided as context for the formulation of hypotheses investigated herein.

1.2. Brain waves

EEG signals are believed to be generated largely by synaptic current sources which, in turn, can be characterized as a global field of synaptic action defined as the number of excitatory or inhibitory synapses that are active at any given time. In the framework presented in (Nunez, 1974; Nunez and Srinivasan, 2006b), signal modulation in the global synaptic action field is not only descriptive, it is postulated to facilitate interactions between remote and perhaps even unconnected cell assemblies. It is thus a top-down mechanism by which the collective behavior of large numbers of separate cell assemblies influences the behaviors of individual assembly. This is analogous to the general behaviors (laws, norms, customs) of a society which have top-down influences on its constitutive members; the latter in turn have combined, bottom-up, influences (e.g., lobbying, voting, protests) on society. Such top-down/bottom-up interactions are referred to as circular causality (Haken, 1999).

In this theory, modulation of the global synaptic action field is considered to be composed partly of waves. This concept of waves has to be understood as in the physical sciences. For example, in the present case, brain waves, could be understood as an oscillation in the global synaptic action field that moves through the brain tissue with minimal loss of energy and displacement of electrical charges. Such wave-like dynamics in the EEG has been reported by many research teams, for example by Massimini et al. (2004) in the case of sleep slow oscillations.

It should be noted that there are no incompatibilities between the wave-like behavior of synaptic activity and the neural functions embedded in cortical and thalamocortical networks, as

the former are large-scale actions working in synergy with the latter, smaller-scale, actions. There is thus no need to oppose these views (Nunez and Srinivasan, 2006a). However, EEG signals preferentially represent larger-scale brain activity (e.g., wave-like behaviors) over smaller-scale network-oriented activity. This is a consequence of the space averaging caused by volume conduction that results from the low conductivity of the skull and the physical separation of neural sources and EEG electrodes (Nunez and Srinivasan, 2006b).

Nunez and Srinivasan (2006b) see specific networks as underlying specific behaviors and cognitive processes. The global fields in which these networks are embedded and participate act top-down on these same networks to produce seemingly unified behaviors and consciousness, phenomena the authors refer to as “brain binding”. This association between brain waves and higher behavioral faculties such as consciousness parallels nicely the hypothesized associations between sleep spindles (herein hypothesized as a brain wave) and various cognitive, mnemonic and personality factors.

1.3. Research goals

Four research questions related to validation of the spindle propagation assessment approach developed in (O'Reilly and Nielsen, 2013a) are investigated in this paper. These questions are:

1) Does the propagation of sleep spindles display organized activity patterns, as opposed to random activity? Given the novelty of this methodology, one might argue that it is essentially assessing random activity instead of a genuine phenomenon. Although by no means a complete validation of the approach, the observation of systematic and coherent patterns of propagation (e.g., hemispherically symmetrical patterns, systematic propagation directions) nonetheless supports the claim that this methodology measures meaningful properties of sleep spindles.

2) Are the propagation properties of spindles best modeled as wave-like activity or as an artifact of spindle activity propagating along axonal pathways? In line with Nunez and Srinivasan (2006b), we propose that the propagation of EEG spindles primarily reflects traveling waves in synaptic action potential fields rather than the properties of signal propagation along axonal pathways of neural networks.

3) Do spindle propagation properties correlate with established spindle characteristics such as amplitude and frequency? Knowing whether propagation properties are very closely related to other features such as spindle amplitude or frequency will inform us about whether the propagation assessment brings redundant or complementary information about spindle generation processes.

4) How reliable is the propagation measure within and between recording nights and subjects? Some spindle properties have been shown to be very reliable within subjects. Determining what nested factors (recording night, subject, recording channel, etc.) have the most influence on propagation properties is essential for using spindle propagation as a potential marker of subject states (i.e., within subject) or traits (i.e., between subjects), or as an investigative tool for understanding general brain neurobiology.

2. Methods

2.1. Experimental protocol

Thirteen women (26 ± 5.7 SD years) and four men (23 ± 4.4 SD years) with no self-reported history of psychiatric illness or sleep problems and in good physical health slept for two

consecutive nights in the sleep laboratory. They were fitted with a 19-electrode montage (Fp1, Fp2,F3, F4, F7, F8, C3, C4, P3, P4, O1, O2, T3, T4, T5, T6, Fz, Cz, and Pz), manually measured and attached with electrode paste, according to the international 10–20 system as well as EOG, EMG, ECG, and respiration leads. Ear electrodes linked with a 10-kΩ resistor were used as reference electrode.

Results from the second laboratory night were not available for two subjects, leaving a total of 32 recording nights for analysis. On the first night, subjects answered a battery of personality questionnaires before electrode placement, including the Sixteen Personality Factor Questionnaire, the Eysenck Personality Inventory, the Beck Depression Inventory, and the Toronto Alexithymia Scale. About 30 minutes before going to sleep, subjects performed an in-house test to evaluate their capacity to remember the elements of a story, the Tower of Hanoi test, and the Corsi block-tapping test. On both nights, subjects were awakened for dream collection during two stage 2 (N2) sleep and two rapid eye movement (REM) sleep episodes. They were awakened with a non-stressful 500 Hz tone (slowly ramped from 50 to 80 dB). Results from questionnaires, memory tests, and dream reports are not further analyzed here. The protocol was approved by the hospital Ethics Review Board and written informed consent was obtained.

2.2. EEG recording and sleep staging

EEG channels were sampled at 128 Hz using a Grass 12 Neurodata acquisition system (-6dB filters with cutoffs at 0.30 and 100 Hz and with a time constant of 0.4 seconds) and were digitally archived. On might notice that this 100 Hz cutoff is higher than the Nyquist frequency

(64 Hz). Hence there is folding of the 64-100 Hz frequency band to the 28-64 Hz band. However, since we are only interested in the 11-16 Hz band in this investigation, aliasing should not influence our analyses. Nights were manually scored for sleep stages by expert polysomnographers according to AASM guidelines (Iber et al., 2007) using the Harmonie software suite (Stellate Systems, Inc., Montreal, Canada). After manual stage scoring, nights were automatically divided into sleep cycles according to the rules suggested by Aeschbach and Borbely (1993).

The assessment of spindle propagation requires sleep spindles to be identified on every recording channel. Here, spindles were automatically detected following an algorithm similar to one adopted by many researchers in the domain (Clemens et al., 2005; Molle et al., 2002; Schabus et al., 2007) and initially proposed by Schimicek et al. (1994). First, raw EEG signals for each channel were filtered using a 511th order band-pass filter with a finite impulse response (FIR) having a rectangular window and -3 dB cutoff frequencies at 11.1 and 14.9 Hz. Possible spindle duration was set to be between 0.5 and 20 seconds. Spindle detection was performed only on signals from sleep stages N2 and N3. As spindle amplitudes vary across subjects and within recording nights, individual thresholds for spindle identification were computed for every sleep cycle of every subject. This threshold was set to the 95th percentile of the distribution of the root mean square (RMS) amplitude, computed for every 0.1-second epoch of stage N2 and N3 of the sleep cycle.

2.3. Spindle characteristics

To compare the propagation delays with other spindle variables, we consider five additional spindle characteristics: density, average frequency, frequency slope, duration, and RMS amplitude. Density is calculated as the number of spindles per minute. Duration and amplitude

of single spindles are obtained directly from the automatic detection procedure whereas the evaluation of spindle propagation delay is described in detail in (O'Reilly and Nielsen, 2013a).

To compute the frequency average and slope, the S-transform (ST)

$$S(t,f) \stackrel{\text{def}}{=} \int_{-\infty}^{+\infty} h(\tau) \frac{|f|}{\sqrt{2\pi}} e^{-\frac{(t-\tau)^2 f^2}{2}} e^{-i2\pi f\tau} d\tau \quad (1)$$

of the spindle-bearing EEG signal $h(\tau)$ is used to compute the time-frequency representation of spindle activity (shown as a color map in Figure 1). Then, for every discrete value on the time axis t of this transform, the mean along the frequency axis is computed with

$$f_{mean}(t) \stackrel{\text{def}}{=} \frac{\int_{-\infty}^{+\infty} f|S(t,f)|df}{\int_{-\infty}^{+\infty} |S(t,f)|df} \quad (2)$$

where $|S(t,f)|$ is the estimated energy amplitude at frequency f and time t. A linear regression of $f_{mean}(t)$ on t over the time window of the spindle duration is computed. The slope of this regression is used as the spindle frequency slope and the spindle frequency average is computed as the value of this regression line at the midpoint of the spindle duration window. Both $f_{mean}(t)$ and the regression line are shown in Figure 1, as the white and the magenta dashed lines respectively.

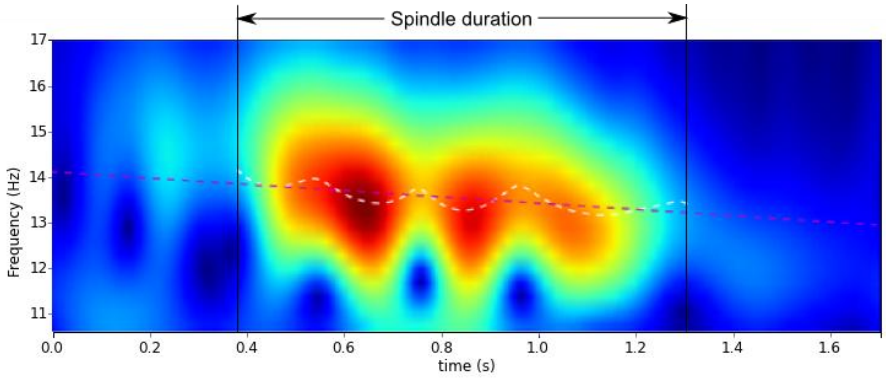

Figure 1. Computation of spindle frequency slope from a linear regression (dashed pink line) of $f_{mean}(t)$ (white line) over time.

In sum, we calculated six primary measures of 3 different types. Spindle duration, average frequency, frequency slope, and RMS amplitude we refer to as point (or monopolar) measurements as they are computed from a measure spatially localized at a single position. Density, in contrast, is not determined for every spindle but is a global variable measured as a property of a recording interval (i.e., spindles have no intrinsic density property, only recording epochs do). Finally, we refer to spindle propagation delay as a relational (or bipolar) measurement because it is computed using information from two spatial locations, i.e., defines a characteristic that relates the activity at these two locations to one another.

2.4. Statistical analysis

We employ multilevel modeling (Hox, 2009) to assess relationships between variables associated with different hierarchical levels such as spindle, electrode and subject properties. This approach avoids problems of intra-class correlation (e.g., spindle properties being more similar within- than between-subjects). A less flexible approach is to average spindle properties by subject to compare variables at the same hierarchical level but this precludes taking into account some other sleep spindle properties such as time of occurrence, duration, or average frequency as co-variables. Multilevel models can be treated easily within the *R* statistical framework as regular mixed models using the *lme4* package (Bates et al.).

Many hierarchical modeling structures are possible for spindle property analyses; Figure 2 shows one of the most complete. It considers five levels: subjects (I), who may have many

recording nights (II), each having many reference channels[1] (III), which are compared to many test channels (IV), and each recording many spindles (V). Importantly, in this design channels are considered to be nested rather than crossed. Whereas crossed factors postulate that electrodes are independent of the subject, nested factors consider them to vary from subject to subject. Since a significantly better fit was obtained with nested channel factors than with crossed factors, the nested approach was adopted.

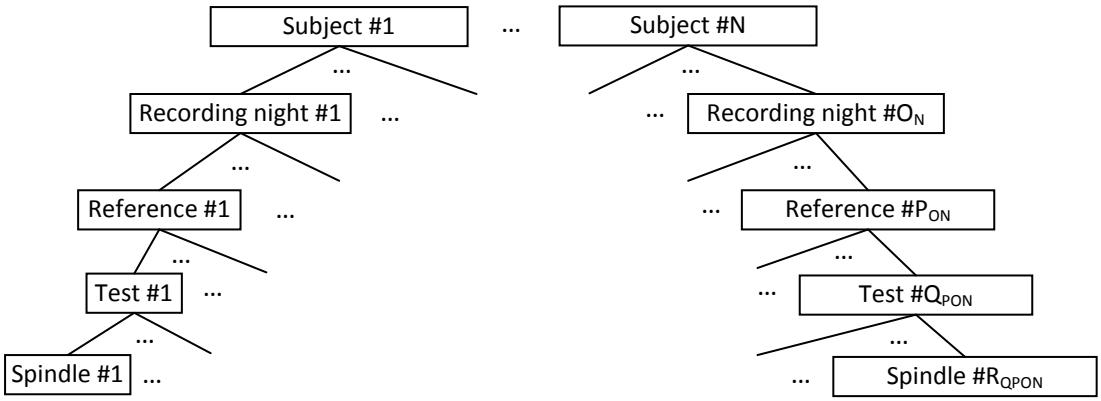

Figure 2. Tree representation of a hierarchical modeling of sleep spindles.

The computation of many statistics typical for ANOVA and linear regression is controversial with such mixed models. This is the case for the p-value whose usefulness in mixed models is a matter of debate in the statistical literature. Debates between renowned statistical

[1] Reference channel should not be confused with reference electrode. The latter is used to determine a reference potential, i.e., to compute the voltage differential between an active electrode and the reference electrode. The former refers to activity on a given channel that is compared to activity on a test channel to assess whether there was propagation of an EEG spindle from the reference channel to the test channel (see O'Reilly C, Nielsen T. Assessing EEG sleep spindle propagation. Part 1: Theory and proposed methodology. Submitted to Journal Of Neuroscience Methods, 2013a. for more details on this topic).

package developers can be viewed in technical forums and by mailing lists (e.g., see Moore, 2010). See also (Johansson, 2011) concerning the general usefulness of p-values.

Given such difficulties, a likelihood approach was chosen for assessing statistical evidence. The likelihood ratio between a model representing a null model (m_0) and an alternative model (m_1) represents the likelihood that m_1 better represents the variability of response variables than does m_0. A likelihood ratio $\frac{L_0}{L_1} = k < 1$ with L_0 and L_1 being respectively the likelihood of m_0 and m_1, provides evidence supporting the alternative model over the null one.

However, to adjust for the different number of parameters in both models, we rather use the relative likelihood (RL) ratio

$$RL = exp\left(\frac{AIC(m_1) - AIC(m_0)}{2}\right) = ke^{p_1 - p_0} \quad (3)$$

where AIC stands for the Akaike Information Criterion, and p_0 and p_1 are respectively the number of parameters in m_0 and m_1. Although likelihood ratios are less common than p-values, they are nevertheless widely adopted and well-documented (see, for example, a tutorial by Blume (2002)).

When reporting likelihood ratios, we will also consider two commonly used threshold values to decide on the importance of the reported evidence: $k = 1/8$ and $k = 1/32$, which are respectively indicators of "fairly strong" and "strong" evidence (Massimini et al., 2004). Note that applying these thresholds to RL rather than to k results in more conservative decisions, as it weights the evidence in favor of larger models.

The coefficient of determination (R^2) is another concept that can be applied to mixed models in various ways. Here, we adopt the definition proposed by (Magee, 1990)and reformulated by Kramer (2005) as

$$R^2_{LR} = 1 - exp\left(-\frac{2}{n}\big(log(L_1) - log(L_0)\big)\right) = ke^{p_1 - p_0} \quad (4)$$

where n is the total number of observations.

3. Results

3.1. Propagation patterns

3.1.1. Relation of propagation direction to spindle characteristics

Point characteristics of spindles recorded on a reference channel were found to be statistically different depending on their propagation direction. Figure 3 shows an example of this computed for the spindles of a typical subject recorded over Cz propagating toward the eight adjacent test electrodes (Fz, F3, C3, P3, Pz, P4, C4, F4). It depicts the average slope of spindle frequency with whiskers spanning the 95% confidence interval.

The non-overlapping confidence intervals between some electrodes in Figure 3 (e.g., P3, P4) indicate that these averaged frequency slopes vary significantly from one test channel to the others. Also, Figure 3 reveals a substantial lateralization, with left-side electrodes (F3, C3, P3) having slopes significantly more negative than their right-side counterparts (F4, C4, P4). There is also a posterior/anterior difference with anterior electrodes showing higher values than posterior electrodes, i.e., Fz > Pz, F3 > P3, and F4 > P4. Finally, Figure 3 reveals that the pattern of frequency slopes as function of propagation direction is highly reproducible from Night 1 (solid lines) to Night 2 (dashed lines) within the same subject.

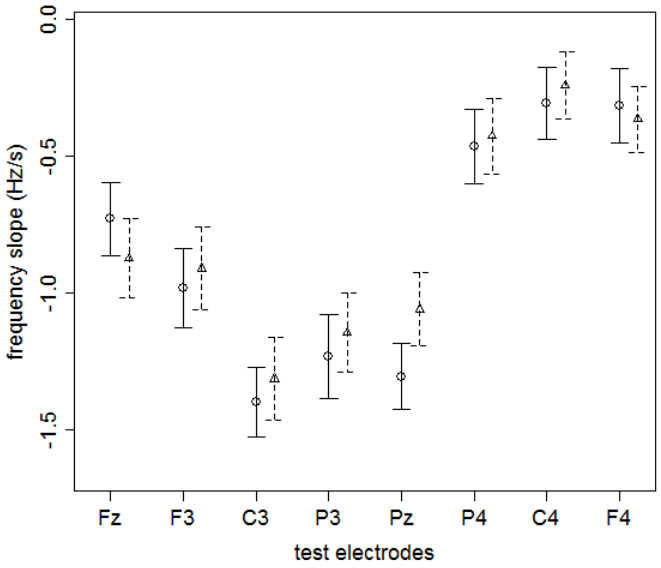

Figure 3. Example of variation in the average spindle frequency slope as function of propagation direction. Slopes near 0.0 signify spindles for which average frequency does not change over time; negative slopes signify spindles that decelerate in frequency. Values are computed for a typical subject using Cz as reference channel and adjacent electrodes as test channels. High inter-night consistencies are apparent for all electrodes except Pz in values displayed for recording night 1 (solid lines) and night 2 (dashed lines).

We computed Spearman's rank correlation coefficients to further characterize this reproducibility for the frequency slope, but also for the average frequency, the propagation delay, and the RMS amplitude. As an example, for the within subject reliability of the average frequency slopes shown in Figure 3, the eight component vectors (one element for each propagation direction) obtained for the first recording night was correlated with the equivalent vector obtained for the second night. These correlations were evaluated for every subject and their mean and standard deviations (SD) computed. The same procedure was also followed for every pair of recording nights taken from different subjects to evaluate the mean and SD of between subject correlations. Resulting statistics are reported in Table 1.

	Within subject		Between subject	
characteristics	mean	SD	mean	SD
Average frequency	0.90	0.07	0.78	0.16
Frequency slope	0.86	0.09	0.84	0.09
Propagation delay	0.79	0.16	0.70	0.21
RMS amplitude	0.72	0.28	0.45	0.40

Table 1. Spearman's rank correlation coefficients illustrating reproducibility of the impact of propagation direction on spindle characteristics within and between subjects. See text for explanation of how these correlations are computed.

The table illustrates very high correlations within subjects (0.72-0.90) and only somewhat lower correlations between subjects (0.45-0.84). This indicates—at least for this modestly sized sample of healthy individuals—that the relationships between propagation direction and spindle characteristics are very stable within subjects, but that a substantial part of this stability is likely attributable to the general neurobiology of the human brain.

3.1.2. Patterns of propagation direction

Combining spindle propagations on the reference channel Cz of all subjects, we assessed the relative proportion of various propagation patterns between reference channel Cz and its adjacent electrodes. Considering eight binary variables indicating only whether or not there was propagation toward each of the eight electrodes, there is $2^8 = 256$ possible propagation patterns. Figure 4 shows the twenty most frequent propagation patterns. Together, they account for 64% of all recorded spindles propagations from Cz. It is also the case that the eight most frequent patterns, accounting for more than 40% of all propagations, are those propagating in a single direction. This indicates that spindle propagation is not a diffuse and

omnidirectional phenomenon, but rather a directed and localized one. It also supports the idea that these recorded propagations are not due to omnidirectional volume conduction.

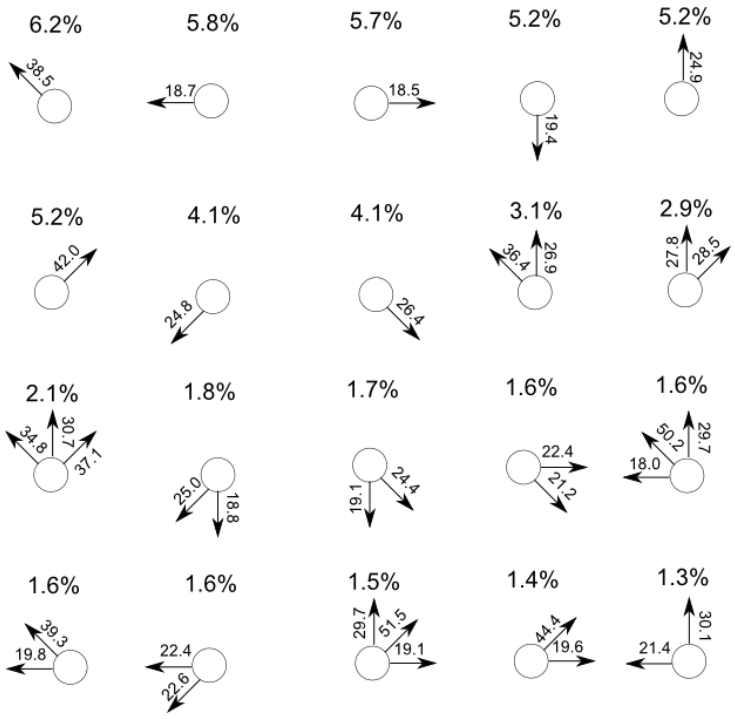

Figure 4. Twenty most frequent spindle propagation patterns from the Cz reference channel with their frequencies of occurrence (all nights combined). Arrows indicate the direction of propagation. Average propagation delays are indicated (in ms) next to the arrows. Together, these accounted for 64% of all recorded spindle propagation patterns.

As discussed previously, point characteristics are dependent on the direction of spindle propagation. To reduce the 256 patterns of propagation to a smaller and more manageable subset, we determined whether the 248 compound patterns (with more than one propagation direction) can be approximated as a linear combination of the 8 elementary patterns (with only one propagation direction). That is, we determined if the mean value of a characteristic of interest assessed for a compound pattern (C_c) was approximated as $C_c \approx \widetilde{C_c} = \frac{\sum_{i=1}^{N} C_{pi} p_i}{\sum_{i=1}^{N} p_i}$ where C_{pi} is the mean value of the characteristic for the i[th] elementary pattern and p_i is a binary

variable indicating if the propagation direction of the i[th] elementary pattern is part of the compound pattern. Table 2 reports values of the characteristics (i.e., spindle average frequency, frequency slope, propagation delay, RMS amplitude) for the elementary patterns (C_{pi}). For example, for the first compound pattern of Figure 4 (Cz toward F3 and Fz), the proposed approximation would predict an average frequency of $\frac{(13.21 + 13.37)}{2} = 13.29$ Hz.

Test electrode	Number of spindles	Average frequency	Frequency slope	Propagation delay	RMS amplitude
F3	1606	13.21	-1.311	0.0380	11.08
C4	1597	13.87	-0.785	0.0175	10.59
C3	1594	13.82	-0.712	0.0185	10.33
Fz	1350	13.37	-1.267	0.0245	11.89
F4	1343	13.26	-1.344	0.0506	11.26
Pz	1336	14.17	-0.300	0.0194	12.43
P3	1078	14.13	-0.068	0.0253	9.87
P4	1071	14.05	-0.217	0.0274	9.56

Table 2. Number of spindles and average values of principal characteristics (average frequency, frequency slope, propagation delay, RMS amplitude) for eight elementary propagation patterns.

Table 3 reports the coefficient of determination (R^2) for modeling the average value of the spindle characteristics for the 248 compound patterns (C_c) with a linear regression of the predicted value ($\widetilde{C_c}$), weighting for the number of spindles observed for every compound pattern.

	Average frequency	Frequency slope	Propagation delay	RMS amplitude
R^2	0.83	0.73	0.69	0.17

Table 3. Modeling accuracy of average spindle characteristics for compound patterns when using a linear combination of the mean characteristics computed on elementary patterns.

As can be seen, this linear composition hypothesis is relatively accurate for most of the characteristics, except RMS amplitude.

3.1.3. Spindle propagation topography

To further validate the extent to which our methodology assesses non-random propagation patterns, we assessed propagation topography. Figure 5 displays a multi-panel portrait of spindle propagation delays using topographic maps for each reference electrode. The color gradient shows average propagation delays computed from the reference electrode for that panel (e.g., Fp1) to all other electrodes; hotter colors reflect lower propagation delay estimates while paler colors (at any delay) reflect lower confidence in estimates.

In Figure 5, highly symmetric patterns of propagation delays are apparent (e.g., F3 versus F4, C3 versus C4, P3 versus P4) as is the fact that only relatively local spindle propagation delays can be assessed with a high degree of confidence. This figure complements preliminary observations reported in (O'Reilly and Nielsen, 2013b) and summarized here: 1) highly symmetrical lateralized patterns of propagation; 2) very close relationships (high positive correlations) between propagation delays and the number of spindle propagations; 3) generally slower propagation delays toward frontal electrodes than toward posterior electrodes possibly supporting the observation of Andrillon et al. (2011) of increasing propagation delays with more anterior (vs. posterior) regions of the brain; 4) larger posterior-to-anterior predominance in propagation direction (i.e., direction of larger delays and of more numerous propagations) the more frontal electrodes are (this tendency decreases for posterior electrodes and even reverses for parietal electrodes); 5) a tendency in the coronal axis for more spindles to propagate, and with larger delays, from central to lateral locations.

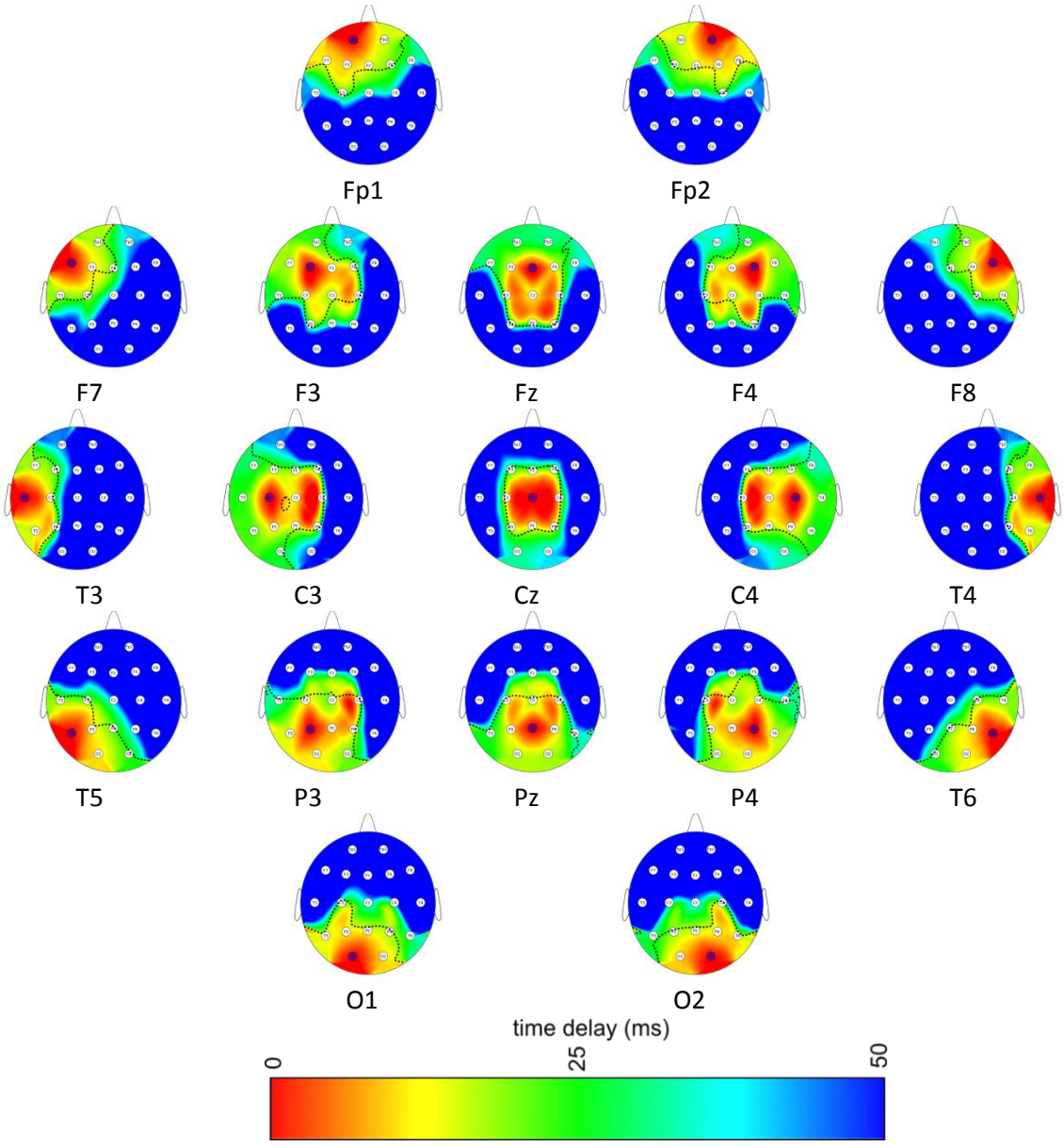

Figure 5. Partition of propagation delays across the scalp for each reference electrode. Hotter colors reflect shorter propagation delays. The dotted line on each map indicates where $\overline{\mathbf{sd}(\boldsymbol{\Delta}_{\mathbf{t}}^{*})} = \mathbf{28.8}$ ms (see O'Reilly and Nielsen (2013a) for details on computation of this empirical threshold) and delineates the region of high confidence in the estimated time delays.

3.2. Transient wave-like properties of sleep spindles

Figure 5 depicts spindle propagation as being a mostly continuous and local phenomenon. No "leaps" of propagation were recorded, as might have been expected if EEG spindles had been propagated deeper in the brain through axonal pathways, emerging on the scalp at various proximal and distal locations. To characterize more rigorously this assertion, we evaluated the proportion of active propagation relationships observed out of the total number of possible relationships, for different inter-electrode distances. We defined this such that adjacent electrodes are considered as separated by a distance of one, the next closest electrodes by a distance of two, and so on to a maximum distance of 4 (see Figure 6).

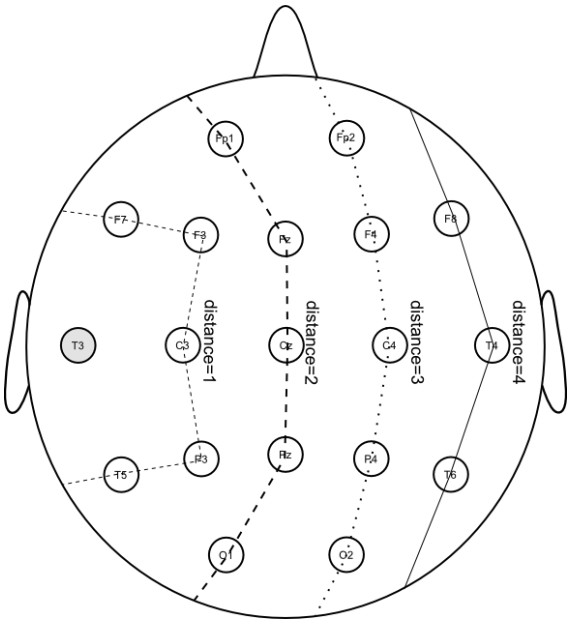

Figure 6. Illustration of how the distance between electrode pairs is defined, using as example possible distances between reference channel T3 and all other test channels.

Defined this way, distance is an integer that can take values between 1 and 4 for our current montage. Table 4 summarizes how this metric reveals the primarily localized nature of sleep spindle propagation. In the first line of the table, the 3774 relationships between pairs of

electrodes for which average propagation delays ($\overline{\Delta_t^*}$) were valid (i.e., were not rejected according to the criteria described in O'Reilly and Nielsen (2013a)) are separated into four classes according to the distance metric. The second line shows the total number of different pairs of channels in our electrode montage, categorized by their distance. In these counts, both (x,y) and (y,x) pairs are considered because they imply inverse propagation directions. The proportion of valid propagations observed for each of these four distances is then computed by dividing the first row by the second and dividing once more by the number of recording nights—32 in this case. The bulk of the observed propagations is for short distances, i.e., between two immediately adjacent electrodes.

Distance metric value	1	2	3	4
Number of valid $\overline{\Delta_t^*}$	2796	802	140	36
Number of different pairs	104	128	88	22
Valid propagation (%)	84.0	19.6	5.0	5.1

Table 4. Evaluation of the percentage of valid propagations in relation to the inter-electrode distance metric.

Figure 7 gives a complementary portrait of this situation depicting the proportion of propagation relationships observed for electrode pairs with valid propagation observations on at least a certain number of nights (varies from 1 to 32). Considering only pairs for which valid propagations were observed in at least up to five recording nights, propagation is observed between every possible pair of adjacent channels (i.e. distance=1). Propagation on distance=2 is also observed reliably between recording nights for a certain proportion of channel pairs, but very few significant propagations are observed on longer distances.

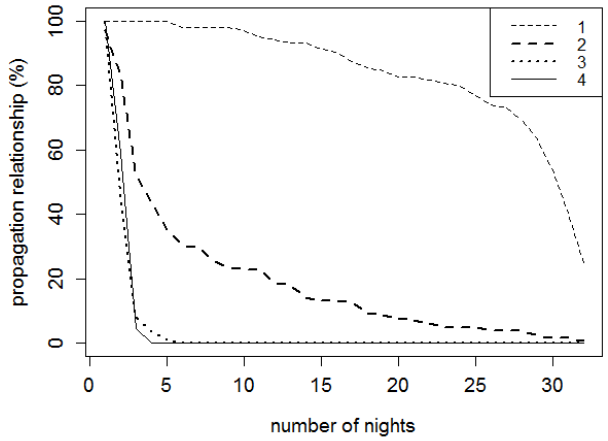

Figure 7. Proportions of valid electrode pairs separated by a distance of between 1 and 4 when considering only pairs for which the mean propagation delay $\overline{\Delta_t^*}$ is valid for at least a certain number of nights (specified as the x-axis value).

Thus, we do not observe long distance propagations which might be expected for brain regions separated spatially but connected anatomically by deep axonal pathways. This supports our view of these EEG propagation patterns as being better modeled as a macro-level portrait of global synaptic potential fields exhibiting transient traveling wave activity. Smaller-scale spindle propagation may also be occurring on preferential neural networks. However, this activity most probably cannot be assessed using EEG recordings since it is thought to be "*biased toward diffusely synchronous spindle generators*" instead of resulting "*from focal asynchronous spindle generators*" as is thought to be the case for the MEG. This is a direct consequence of the cortical area projecting to each sensor being about 25 times larger for EEG recording as for MEG recording (Bonjean et al., 2012).

Our conclusions should also not be confused with those related to functional connectivity. Time- or phase-locked activity between distant brain regions as assessed by various

techniques (e.g., Blinowska, 2011) can indeed exist without implying direct signal propagation (O'Reilly and Nielsen, 2013a). This is particularly true for EEG spindles which show relatively high inter-channel coherence (~0.7) compared, for example, with MEG spindle inter-gradiometer coherence (~0.3) (Bonjean et al., 2012).

Our results also show that EEG spindle propagation appears to share some properties of electromagnetic wave propagation, but at many orders of magnitude slower. Similar to the physic of electromagnetic wave propagation, EEG spindles with lower fundamental frequencies tend to be associated with slower propagation speeds. This tendency can be seen by comparing Figure 8.a and b, which show the variation of average frequency and propagation velocity computed for each reference channel and extrapolated to the entire head[2]. Average frequency and velocity variability display some degree of similarity. This is reflected by a statistically significant ($p = 0.02$) Pearson's coefficient of correlation of $\rho = 0.54$. This correlation even rises up to $\rho = 0.85$ when considering the robust correlation (minimum volume ellipsoid [MVE] algorithm). This relationship also takes into account the direction of propagation as can be seen by Figure 8.c and d which show the average frequency and velocity for spindles propagating between each pair of adjacent electrodes. Here again a substantial correlation is obtained (Pearson: $\rho = 0.61$, $p = 3.7e - 12$; MVE: $\rho = 0.82$).

[2] These results are computed only on 14 subjects. Head dimensions were not available for 3 subjects, making the calculation of velocity from inter-channel delays not possible for them.

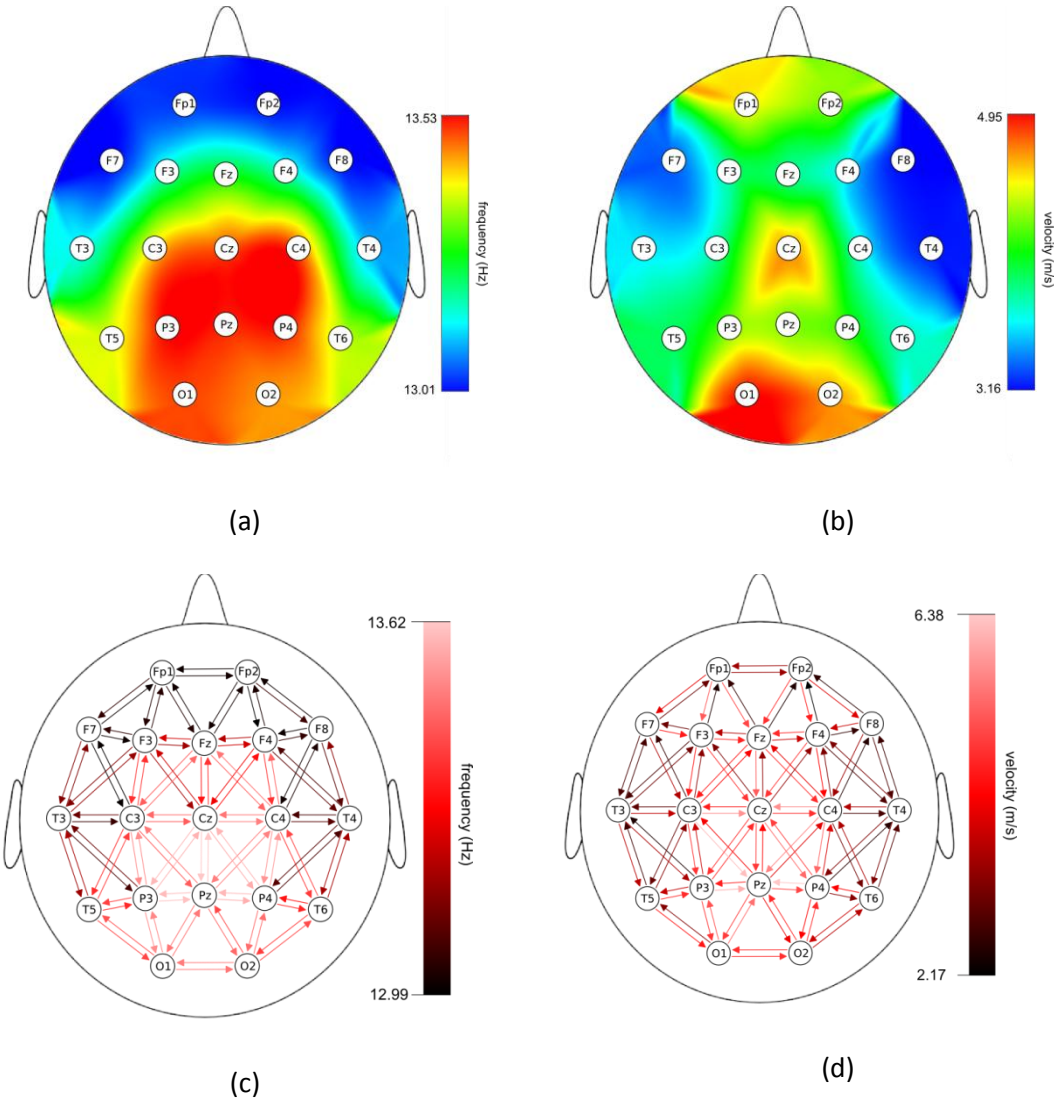

Figure 8. (a,b) Average spindle frequency (a) and propagation velocity (b). Slower spindles (both in frequency and velocity) are observed in frontal regions and faster spindles around the Pz lead. Maps in (c,d) are the same as (a,b) but the information is given for every electrode pair.

To complete this investigation of relationships between spindle average frequency and propagation velocity, Figure 9.a and b respectively show differential propagation delay and the difference in spindle average frequency between pairs of adjacent electrodes, whereas Figure

9.c is a scatter plot linking the results from a and b[3]. From these figures, it can be seen that differential propagation delays are related to the gradient of spindle frequency. High density EEG recordings would be necessary to characterize more precisely the accuracy of this finding but with our data set we obtain relationships between the propagation delay difference ($\Delta\tau$) and the average frequency difference (Δf) that can be approximated by $\Delta f = 60\Delta\tau$. Two distinct clusters of spindle propagation (in blue and green in Figure 9.c) may indicate that spindles over frontal regions are qualitatively distinct from those over the rest of the scalp.

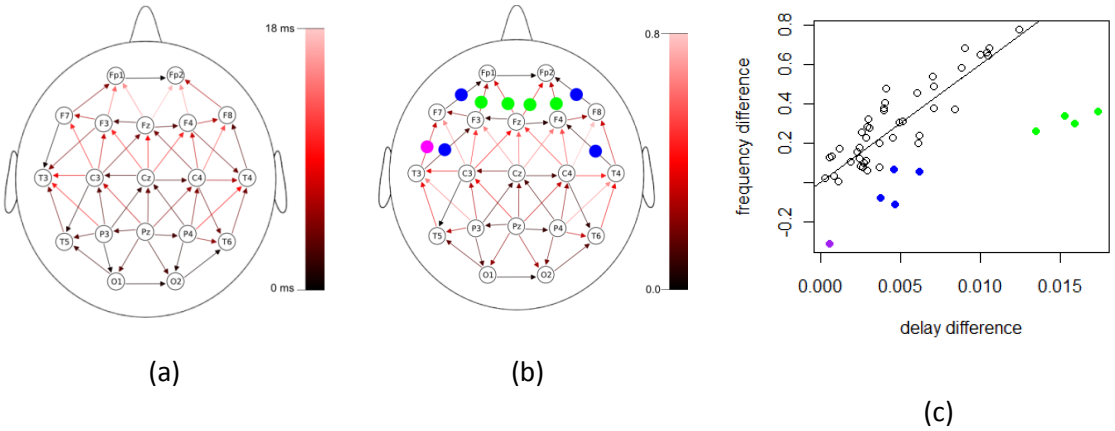

(a) (b) (c)

Figure 9. (a) Differential delays of propagation between every pair of adjacent electrodes. The arrow head indicates the direction of slower propagation whereas the arrow color indicates the magnitude of the differential. (b) Differences in spindle average frequency between adjacent electrodes. This pattern of variability is closely related to the one shown in (a). This resemblance is further described in (c) by a scatter plot linking the differential propagation delay to the spindle average frequency difference. The overall correlation is 0.62 but if we remove the clusters of green and blue points which are associated with specific fronto-temporal regions as well as an outlier (in purple), the correlation climb to 0.90. This outlier is the only relationship in (a) that is not laterally symmetrical. The solid diagonal line shows that relationships between the

[3] As opposed to Figure 8, the results of Figure 9 are computed on all 17 subjects.

delay difference ($\Delta\boldsymbol{\tau}$) and the average frequency difference ($\Delta\boldsymbol{f}$) can be approximated by $\Delta\boldsymbol{f} = \mathbf{60}\Delta\boldsymbol{\tau}$.

3.3. Correlation with other spindle characteristics

Spearman's correlation coefficients between different spindle characteristics were computed on the 3774 combinations of recording night, reference channel, and test channel for which a valid value $\overline{\Delta_t^*}$ was obtained. The spindles for which propagation delays Δ_t^* were used for the computation of the median values $\overline{\Delta_t^*}$ were also used for computing the median value of average frequency, frequency slope, duration, and RMS amplitude. The corresponding spindle density was also computed. Table 5 displays the correlation matrix between these different variables.

	Average Frequency	Frequency Slope	Duration	RMS Amplitude	Density
Propagation Delay	-0.01	**-0.29**	0.00	-0.03	**0.13**
Average Frequency		**0.39**	**0.22**	**0.23**	-0.04
Frequency Slope			**0.30**	0.03	**-0.07**
Duration				**0.17**	**0.33**
RMS Amplitude					**0.46**

Table 5. Correlation coefficients (Spearman, N =3774, bold is used for p-value < 0.01) between the principal spindle characteristics.

It should be noted that the computation of point characteristic averages used in this correlational analysis takes into account propagation direction. That is, median values are calculated only on the subset of spindles that propagated from the reference channel to the test channel instead of on all spindles recorded on the reference channel, regardless of propagation properties. As shown in Table 5, propagation delay furnishes novel information, i.e., the measure is relatively poorly correlated with other spindle characteristics.

3.4. Sources of variability

As discussed in section 2.4, there may be advantages to a multilevel modeling of spindle characteristics taking into account individual spindles rather than averages. This would allow assessment of property correlations at the spindle level, e.g., correlations between spindle amplitude and the timing of their occurrence within the night. However, this approach would necessitate computing models on very large numbers of observations—more than 600,000 in the present case. An alternative is to model some aggregated value of a spindle characteristic. For example, one might consider computing the median value of a spindle characteristic for each different sleep stage of each REM/NREM cycle. Such grouping would enable the study of spindle relative timing within the night (e.g., roughly measured as the sleep cycle) and the sleep stage. In our case, this type of aggregation reduces the number of observation to a more manageable 24,045. Preliminary work (unpublished) suggests generally similar results are produced by both modeling approaches. Thus, we chose the second, less computationally demanding, approach to assess our results.

In Table 6, $RL < 1E-100$ are indicated as being zeros. Also, density was computed only for the whole nights, not for individual sleep cycles which is why the impact of cycle is not available (N/A) for this variable. Bold characters were used to indicate “fairly strong” evidence that the factor is significant whereas cells were colored grey when this evidence was “strong”. For each row, the coefficient of determination of the model including all previous significant parameters is given. For example, using the notation used by the *lme4* package of the statistical software *R*, the $R^2_{LR} = 0.45$ given for the last row of the *Propagation delay* column is computed for the following model: $delay \sim 1 + (1|subject) + (1|night) + (1|ref) + (1|test) +$

$cycle$. In this model, $test$, ref, $night$, and $subject$ are all nested factors and the $stage$ factor is absent because it has no significant effect as shown by a RL of 1.7.

	Propagation delay		RMS amplitude		Frequency slope		Average frequency		Duration		Density	
	RL	R^2_{LR}	RL	R^2_{LR}	RL	R^2_{LR}	RL	R^2_{LR}	RL	R^2_{LR}	RL	R^2_{LR}
subject	**0.00E+00**	0.03	**0.00E+00**	0.26	**0.00E+00**	0.06	**0.00E+00**	0.21	**0.00E+00**	0.04	**1.08E-78**	0.06
night	**1.88E-70**	0.04	**8.64E-90**	0.27	**4.19E-11**	0.07	**2.79E-31**	0.22	**9.21E-60**	0.05	3.38E-01	0.06
ref.	**0.00E+00**	0.13	**0.00E+00**	0.58	**0.00E+00**	0.17	**0.00E+00**	0.55	**0.00E+00**	0.07	**1.95E-78**	0.11
test	**0.00E+00**	0.44	**0.00E+00**	0.84	**0.00E+00**	0.20	**0.00E+00**	0.70	7.93E-01	0.07	**1.60E-02**	0.11
stage	1.70E+00	0.44	**0.00E+00**	0.85	**4.49E-04**	0.20	**0.00E+00**	0.71	**0.00E+00**	0.13	**0.00E+00**	0.52
cycle	**4.97E-02**	0.45	**3.88E-11**	0.85	6.12E-01	0.20	**0.00E+00**	0.71	1.83E+00	0.13	N/A	N/A

Table 6. Relative likelihood and coefficient of determination for modeling different spindle characteristics (column) with different factors (row): subject uniquely identifies the each participant, night takes a value of 1 or 2 (first or second recording night), ref and test identify the reference and test channels respectively, stage is either N2 or N3 and cycle specifies the sleep cycle (an integer between 1 and 7).

As can be seen from Table 6, much of the variation of duration and frequency slope cannot be accounted for with these factors. A plausible explanation is that experimental error, such as error related to spindle scoring variability, impacts these characteristics. It is not surprising to see low coefficients of determination for the frequency slope since this characteristic is likely affected by spindle duration, the scoring of which has poor reliability (O'Reilly and Nielsen, 2013c).

Also in Table 6, the important impact of sleep stage on sleep spindle density is apparent. Spindle RMS amplitude and average frequency are very well modeled by the factors considered,

with R^2_{LR} of 0.85 and 0.71 respectively. A significant part of propagation delay variability is also captured, but there is apparently room for lowering experimental error or for finding other factors that may raise the R^2_{LR} value of 0.45. Significant outcomes for the *test* factor for spindle RMS amplitude, average frequency, frequency slope, and density suggest that propagation direction influences values of these variables. This does not, however, appear to be the case for spindle duration.

	Propagation delay (ms)	RMS amplitude	Frequency slope	Average frequency	Duration	Density
Overall mean	**21.730**	**8.655**	**-0.2813**	**13.317**	**0.7655**	**1.612**
Residual SD	**16.964**	**1.036**	**0.2976**	**0.120**	**0.0972**	**0.184**
Subject SD	**3.801**	**1.594**	**0.0952**	**0.131**	**0.0171**	**0.093**
Night SD	**4.747**	**0.412**	**0.0000**	**0.032**	**0.0161**	0.000
Ref. SD	**6.730**	**1.785**	**0.1362**	**0.169**	**0.0254**	**0.141**
Test SD	**20.727**	**1.943**	**0.1172**	**0.138**	0.0128	**0.221**
Stage mean	-0.077	**-0.461**	**-0.0148**	**-0.034**	**-0.0505**	**-0.406**
Cycle mean	**0.248**	**0.038**	0.0026	**0.015**	-0.0004	N/A

Table 7. Values of parameters for modeling spindle characteristics (column) with the full model containing every factor (rows). Significance coding as for Table 6. Using mixed modeling, random and fixed factors are associated with standard deviation and mean parameters respectively.

Table 7 shows the modeling parameters computed. For the random factor and the residuals, standard deviations are reported instead of variances because they are on the same scales as mean values, and thus more readily illustrate the impact of each term on the model. The table shows that density and frequency slope are highly stable features over recording nights of individual subjects. Without surprises, for a specific reference channel, the propagation delay depends a lot on the test channel. Propagation delays seem to increase during the night.

This also looks to be the case for the RMS amplitude and the average frequency. In average, the average frequency of the spindles clearly slow down from the beginning of the spindle to its end, with a decrease of about 0.28 Hz per second.

3.5. Reliability

As described in section 3.1.1, spindle characteristics vary depending on propagation direction and their patterns of variation are highly repeatable from one recording night to another for individual subjects, and, to a lesser extent, from one subject to another. This indicates a good reproducibility of propagation characteristics.

To further assess the reliability of propagation delays and to compare it with that of other spindle characteristics, standard deviations were computed between recording nights, within recording nights (i.e., across non-REM sleep periods), and between recording nights/within subjects. The results reported in Table 8 indicate that the variability within recording nights is higher than that between recording nights of individual subjects. This may reflect highly repeatable subject-specific patterns of variability.

	Prop. delay (ms)	RMS amplitude (μV)	Frequency slope (Hz/s)	Average frequency (Hz)	Duration (ms)	Density (spindle/ minute)
Between recording nights	5.33	1.76	0.152	0.171	59.1	0.195
Within recording nights	3.56	0.57	0.138	0.071	72.0	N/A
Between recording nights/within subjects	1.76	0.34	0.047	0.035	47.6	0.106

Table 8. Estimated standard deviations between recording nights, within recording nights, and between recording nights/within subjects for different spindle characteristics.

These results are in line with observations that spindle variability patterns are highly subject-specific, much like fingerprints (De Gennaro et al., 2005; Morrow and Casey, 1986). Differences in brain structure are a possible explanatory factor (Tyvaert et al., 2008).

4. Discussion

4.1. Confirmation of the methodology

The results presented here converge with those described in (O'Reilly and Nielsen, 2013a, b) in providing strong support for the general validity and reliability of the proposed methodology in several respects. First, we observed clear patterns of propagation (i.e., from posterior to anterior and from central to lateral) that are repeatable, coherent from electrode to electrode, and highly symmetrical for left and right hemispheres. Second, statistics used within this framework are very robust, and hence repeatable, as they are computed using large numbers of spindles for each whole-night polysomnogram (on average 501 ± 146 [SD] per channel, per night). Third, the four rejection criteria used within the approach ensure reliable estimates at each step of the process (O'Reilly and Nielsen, 2013a). Fourth, many of our observations are in agreement with those of other research teams. For example, the measures reported in Figure 7 replicate reported reductions of spindle average frequency from caudal to rostral regions (Peter-Derex et al., 2012) and a topographic distinction between slow (9-12 Hz) frontal and fast (13-16 Hz) centroparietal spindle frequencies (Andrillon et al., 2011; De Gennaro and Ferrara, 2003; Jankel and Niedermeyer, 1985; Jobert et al., 1992). The latter distinction is also supported by an apparently distinct cluster of spindles with unique properties located in the frontal region, as shown in Figure 8.

4.2. Local propagation of sleep spindles

We assessed only local propagation of sleep spindles. This may be related to the local nature of sleep spindles reported by some authors (Andrillon et al., 2011; Nir et al., 2011). However, further study is needed before drawing firm conclusions on this similarity in findings for two main reasons. First, spindle propagation reported in these other studies is assessed on much larger time intervals—the authors associate spindles detected on different channels as soon as there is a time overlap—and without regard to differences in spindle frequency from channel to channel. Further, in these studies locality is accounted for by the percentage of monitored brain structure that expresses spindle activity (with implanted electrode recordings).

Second, the non-observation of longer distance spindle propagations in the present study may be related to properties of the methodology: 1) the use of a too-small maximal propagation delay Δ_w for the comparison of activity between recording channels does not allow for sufficiently confident assessments of average propagation delays that are much larger than 25 ms (O'Reilly and Nielsen, 2013a); 2) the metric used for measuring signal similarity does not match spindles with different amplitudes such that only local propagation would be observed if spindles were decreasing in amplitude as they propagate. Thus, larger values of Δ_w and a more flexible approach in regards of spindle amplitude[4] could be tested in future works to confirm whether or not the algorithm is applicable to assessing wider spindle propagation fields. Nevertheless, as stated previously, no large distance propagations or "leaps" of spindles from one anatomical region to another were observed within this 25 ms window.

4.3. Sleep spindles as a wave-like activity

[4] The approach allows for such a modification by simply using a Euclidean instead of an infinite norm in normalization of the similarity index between the activities of different channels (see O'Reilly & Nielsen (2013a) for more details.

Along with this absence of propagation between distant cerebral regions, the observed relationship between spindle average frequency and propagation velocity also support the hypothesis that spindles can be considered brain waves, as defined by Nunez and Srinivasan (2006a). Also supporting this idea is the fact that we observed average posterior-anterior propagation delays of 8 to 28 milliseconds between adjacent electrodes and—once combined with head measurements performed for electrode placements—propagation speeds between 2.3 and 7.0 meter per second (m/s). The latter speeds closely approximate the range of 5 to 10 m/s predicted by Nunez and Srinivasan (2006b). They are also close to the speeds of EEG traveling waves obtained using other methodologies. To illustrate; Massimini et al. (2004) found speeds of 1.2–7.0 m/s for sleep slow oscillations.

It could be argued that nothing allows the differentiation between two possible interpretations for the observed propagations. The first one, defended in the present paper, considers propagation from one recording channel to another to be a wave-like displacement of the global synaptic potential field.

In the second interpretation, the propagation delays observed are the result of signals emitted from a hidden source (not visible from EEG measurements) which propagate to different cortical locations with different axonal propagation delays, causing the spindle to be observed at different cortical locations at different moments. For sleep spindles, such a generator would be localized within or near the thalamus (Ueda et al., 2000). The differential propagation delay in appearance of spindle activity at two cortical locations that are linked to the thalamus by 10 cm and 20 cm axons respectively (fictive numbers but within the size range of normal human brains) should be only in the order of 3 milliseconds, since the conduction

velocity of thalamocortical fibers is about 30 m/s (Kimura et al., 2008).These delays are difficult to reconcile with delays of tens of milliseconds observed in our study.

It should be noted, however, that the mechanism generating this wave-like displacement of the global synaptic potential field could either reside within the cortex or be an artifact from the action of remote latent sources, for example, two time-locked loci within the thalamus generating, with some delay, potentials that are transmitted to adjacent cortical locations.

4.4. Correlations between spindle average frequency and duration

In Table 5, a positive correlation between spindle frequency and duration is reported. This might seem to contradict some studies in which spindle frequency appears to correlate inversely with duration (Crowley et al., 2002; Nicolas et al., 2001), but these studies looked at age-related impacts (duration was shorter and frequency faster with aging). On the other hand, (De Gennaro et al., 2005) reported only a small difference in spindle duration for fast and slow spindles while (Dehghani et al., 2011) showed that spindles might consist of a sequence of a posterior-fast and an anterior-slow component. Thus, duration might vary substantially depending on the definition of sleep spindles considered. Also, we have shown that the scoring approach applied can have a great impact on duration since this characteristic exhibits low reliability between approaches (O'Reilly and Nielsen, 2013c). More investigation seems warranted to clearly define relationships between spindle frequency and duration.

4.5. Open avenues

The present findings raise many questions warranting further study. First, as shown in Figure 3, not only do most spindles decelerate in average frequency over time, but this deceleration is more accentuated for left- than for right-side electrode leads. Although this laterality effect is not pursued here in more detail, the reliability of our observations invites more focused investigation.

Second, as shown in Table 8, spindle propagation is stable from night to night and consistent from one individual to another; this suggests that propagation may relate to stable and trait-like homeostatic, cognitive, or functional characteristics. However, night-to-night responses of propagation characteristics to challenges such as sleep disruption and learning tasks remain to be investigated. So do changes in propagation as a function of developmental milestones and aging more generally.

4.6. Possible methodological alternatives

Given the absence of discontinuous spindle propagation over the scalp as shown in Figure 5, it might be more convenient to compute propagation only between adjacent channels than between every pair of channels. This approach is appealing for two reasons. First, it is much less computationally intensive and produces results that are easier to plot and interpret. Moreover, it might be the only reasonable approach if this methodology is to be applied to large electrode arrays such as in high-density EEG recordings. Second, for between-groups statistical analyses, it might be necessary to limit the number of analyzed propagation relationships to minimize the reduction in power introduced by adjusting for very large number of comparisons (e.g.,

Bonferroni correction, random fields). For this reason, it is common in neuroimagery to see the use of regions of interest to limit the number of comparisons, a procedure similar to what we are proposing by studying only relationships between adjacent electrodes (i.e., both share the idea of limiting investigation only to the most promising relationships). Nonetheless, as noted previously, some validational work using all electrode pairs, higher Δ_w values, and amplitude-flexible spindle comparisons are still needed to rule out the possibility of larger-scale propagations with larger propagation delays.

4.7. Limitations

The various experimental manipulations (e.g., neuropsychological testing) and sleep disturbances (e.g., night awakenings for dream report collection) might have influenced characteristics of the spindles assessed in this study. This would be expected from evidence cited earlier that sleep spindle characteristics are altered by new learning situations. This eventuality limits the extent to which the present results may be compared with spindle characteristics assessed using different experimental setups. However, this limitation is in no way an obstacle to validating the spindle propagation methodology per se.

A second limitation of the present study is the spindle detection algorithm upon which the propagation method is based. Validity of the latter can only be as good as that of its accompanying the spindle detection technique. And as there continue to be important difficulties in achieving consensus on how to detect sleep spindles—including on what exactly is and is not a sleep spindle—there will inevitably remain uncertainty about the assessment of spindle characteristics. At present, a conservative way forward is to confront these assessments using different spindle definitions and classification schemes. For example, spindles could be

defined as a single class of events or as several classes, such as slow and fast spindles. Similarly, spindles might be classified by systems that use different detection strategies. These variations in methodological framework could highlight patterns of differences and similarities such that we may distinguish between robust (i.e., observed regardless of the methodology) and volatile (i.e., observed inconsistently from one paradigm to another) findings. Such an investigation could provide valuable insights to better characterized regularities in the spindle phenomenon and build a more valid and consensual basis for its definition.

Also, although the within and between subject repeatability of our results was relatively strong, we cannot rule out every type of systematic error. Corroboration of the work using other techniques, such as intracranial recording, is needed.

5. Conclusion

The present work describes the application of a methodology for characterizing the propagation of EEG sleep spindles using laboratory sleep recordings. Results indicate that the method detects non-random propagation of activity over multiple recording channels and that this propagation is more consistent with wave-like activity than it is with neuronal transmission. The results also indicate that spindle propagation correlates with density and frequency slope, but not with spindle average frequency, duration, and RMS amplitude. Finally, the results demonstrate that the propagation of spindles is a reliable measure within and between both nights and subjects.

The work agrees at many points with alternative approaches documented in the literature. Nonetheless, it is new and much remains to be explored. There is a particular need

for studies investigating the functional relevance of propagation characteristics, e.g., the assessment of relationships between propagation features and subject demographics (age, gender), cognitive variables (scores on learning tests, age-related decline), sleep architecture (sleep efficiency, sleep homeostasis), and patient diagnoses (schizophrenia, epilepsy). Comparative studies with other spindle analysis techniques (e.g., coherence) are also needed to further validate the approach, to evaluate its potential complementarities with other approaches, and to thereby accelerate discovery among researchers in this important frontier of brain science.

Acknowledgements

The authors thank Gaétan Poirier for implementing the automatic spindle detection algorithm described in section 2.2. and Tyna Paquette for technical assistance. This research was supported by grants from the Natural Sciences and Engineering Research Council of Canada and the Canadian Institutes of Health Research.

References

Acır N, Güzeliş C. Automatic recognition of sleep spindles in EEG by using artificial neural networks. Expert Syst Appl, 2004; 27: 451-8.

Aeschbach D, Borbely AA. All-night dynamics of the human sleep EEG. J Sleep Res, 1993; 2: 70-81.

Andrillon T, Nir Y, Staba RJ, Ferrarelli F, Cirelli C, Tononi G, Fried I. Sleep spindles in humans: insights from intracranial EEG and unit recordings. J Neurosci, 2011; 31: 17821-34.

Babadi B, McKinney SM, Tarokh V, Ellenbogen JM. DiBa: a data-driven Bayesian algorithm for sleep spindle detection. IEEE Trans Biomed Eng, 2012; 59: 483-93.

Bates D, Maechler M, Bolker B. lme4: Linear mixed-effects models using S4 classes. http://cran.r-project.org/web/packages/lme4/index.html.

Blinowska KJ. Review of the methods of determination of directed connectivity from multichannel data. Med Biol Eng Comput, 2011; 49: 521-9.

Blume JD. Likelihood methods for measuring statistical evidence. Stat. Med., 2002; 21: 2563-99.

Bonjean M, Baker T, Bazhenov M, Cash S, Halgren E, Sejnowski T. Interactions between core and matrix thalamocortical projections in human sleep spindle synchronization. J Neurosci, 2012; 32: 5250-63.

Causa L, Held CM, Causa J, Estevez PA, Perez CA, Chamorro R, Garrido M, Algarin C, Peirano P. Automated sleep-spindle detection in healthy children polysomnograms. IEEE Trans Biomed Eng, 2010; 57: 2135-46.

Clemens Z, Fabo D, Halasz P. Overnight verbal memory retention correlates with the number of sleep spindles. Neuroscience, 2005; 132: 529-35.

Crowley K, Trinder J, Kim Y, Carrington M, Colrain IM. The effects of normal aging on sleep spindle and K-complex production. Clin Neurophysiol, 2002; 113: 1615-22.

De Gennaro L, Ferrara M. Sleep spindles: an overview. Sleep Med Rev, 2003; 7: 423-40.

De Gennaro L, Ferrara M, Vecchio F, Curcio G, Bertini M. An electroencephalographic fingerprint of human sleep. NeuroImage, 2005; 26: 114-22.

Dehghani N, Cash SS, Halgren E. Emergence of synchronous EEG spindles from asynchronous MEG spindles. Hum Brain Mapp, 2011; 32: 2217-27.

Duman F, Erdamar A, Erogul O, Telatar Z, Yetkin S. Efficient sleep spindle detection algorithm with decision tree. Expert Syst Appl, 2009; 36: 9980-5.

Ferrarelli F, Peterson MJ, Sarasso S, Riedner BA, Murphy MJ, Benca RM, Bria P, Kalin NH, Tononi G. Thalamic dysfunction in schizophrenia suggested by whole-night deficits in slow and fast spindles. Am J Psychiatry, 2010; 167: 1339-48.

Fogel SM, Smith CT. The function of the sleep spindle: a physiological index of intelligence and a mechanism for sleep-dependent memory consolidation. Neurosci Biobehav Rev, 2011; 35: 1154-65.

Haken H. What Can Synergetics Contribute to the Understanding of Brain Functioning? In Uhl C, editor. Analysis of Neurophysiological Brain Functioning. Springer Berlin Heidelberg, 1999: 7-40.

Hox JJ. Multilevel analysis : techniques and applications. Psychology Press: New York, 2009.

Huupponen E, Gomez-Herrero G, Saastamoinen A, Varri A, Hasan J, Himanen SL. Development and comparison of four sleep spindle detection methods. Artif Intell Med, 2007; 40: 157-70.

Iber C, Ancoli-Israel S, Chesson a, Quan SF. The AASM Manual for the Scoring of Sleep and Associated Events: Rules, Terminology and Technical Specifications. American Academy of Sleep Medicine: Westchester, IL, 2007.

Jankel WR, Niedermeyer E. Sleep spindles. J Clin Neurophysiol, 1985; 2: 1-35.

Jobert M, Poiseau E, Jahnig P, Schulz H, Kubicki S. Topographical analysis of sleep spindle activity. Neuropsychobiology, 1992; 26: 210-7.

Johansson T. Hail the impossible: p-values, evidence, and likelihood. Scand J Psychol, 2011; 52: 113-25.

Kimura T, Ozaki I, Hashimoto I. Impulse propagation along thalamocortical fibers can be detected magnetically outside the human brain. J Neurosci, 2008; 28: 12535-8.

Kramer M. R2 statistics for mixed models. 17th Annual Kansas State University Conference on Applied Statistics in Agriculture: Manhattan, Kansas, 2005.

Magee L. R2 Measures based on Wald and likelihood ratio joint significance tests. Am Stat, 1990; 44: 250-3.

Massimini M, Huber R, Ferrarelli F, Hill S, Tononi G. The sleep slow oscillation as a traveling wave. J Neurosci, 2004; 24: 6862-70.

Molle M, Bergmann TO, Marshall L, Born J. Fast and slow spindles during the sleep slow oscillation: disparate coalescence and engagement in memory processing. Sleep, 2011; 34: 1411-21.

Molle M, Marshall L, Gais S, Born J. Grouping of spindle activity during slow oscillations in human non-rapid eye movement sleep. J Neurosci, 2002; 22: 10941-7.

Moore C. Linear mixed-effects regression p-values in R: A likelihood ratio test function. http://blog.lib.umn.edu/moor0554/canoemoore/2010/09/lmer_p-values_lrt.html, 2010.

Morrow TJ, Casey KL. A microprocessor device for the real-time detection of synchronized alpha and spindle activity in the EEG. Brain Res Bull, 1986; 16: 439-42.

Nicolas A, Petit D, Rompre S, Montplaisir J. Sleep spindle characteristics in healthy subjects of different age groups. Clin Neurophysiol, 2001; 112: 521-7.

Nir Y, Staba RJ, Andrillon T, Vyazovskiy VV, Cirelli C, Fried I, Tononi G. Regional slow waves and spindles in human sleep. Neuron, 2011; 70: 153-69.

Nunez PL. The brain wave equation: a model for the EEG. Math Biosci, 1974; 21: 279-97.

Nunez PL, Srinivasan R. Electric fields of the brain the neurophysics of EEG, 2nd ed. Oxford University Press: Oxford, 2006a.

Nunez PL, Srinivasan R. A theoretical basis for standing and traveling brain waves measured with human EEG with implications for an integrated consciousness. Clin Neurophysiol, 2006b; 117: 2424-35.

O'Reilly C, Nielsen T. Assessing EEG sleep spindle propagation. Part 1: Theory and proposed methodology. Submitted to J Neurosci Methods, 2013a.

O'Reilly C, Nielsen T. Assessing the propagation of EEG transient activity. The 9th international Workshop on Systems, Signal Processing and their Applications: Special Sessions: Mazafran, Algeria, 2013b: 126-33.

O'Reilly C, Nielsen T. Sleep spindle detection: Automatic detection and evaluation of performance with a fine temporal resolution. Submitted to IEEE Trans Biomed Eng, 2013c.

Peter-Derex L, Comte JC, Mauguiere F, Salin PA. Density and frequency caudo-rostral gradients of sleep spindles recorded in the human cortex. Sleep, 2012; 35: 69-79.

Schabus M, Dang-Vu TT, Albouy G, Balteau E, Boly M, Carrier J, Darsaud A, Degueldre C, Desseilles M, Gais S, Phillips C, Rauchs G, Schnakers C, Sterpenich V, Vandewalle G, Luxen A, Maquet P. Hemodynamic cerebral correlates of sleep spindles during human non-rapid eye movement sleep. Proc Natl Acad Sci U. S. A., 2007; 104: 13164-9.

Schimicek P, Zeitlhofer J, Anderer P, Saletu B. Automatic sleep-spindle detection procedure: aspects of reliability and validity. Clin Electroencephalogr, 1994; 25: 26-9.

Schonwald SV, de Santa-Helena EL, Rossatto R, Chaves ML, Gerhardt GJ. Benchmarking matching pursuit to find sleep spindles. J Neurosci Methods, 2006; 156: 314-21.

Sinha RK. Artificial neural network and wavelet based automated detection of sleep spindles, REM sleep and wake states. J Med Syst, 2008; 32: 291-9.

Tyvaert L, Levan P, Grova C, Dubeau F, Gotman J. Effects of fluctuating physiological rhythms during prolonged EEG-fMRI studies. Clin Neurophysiol, 2008; 119: 2762-74.

Ueda K, Nittono H, Hayashi M, Hori T. Estimation of generator sources of human sleep spindles by dipole tracing method. Psychiatry Clin Neurosci, 2000; 54: 270-1.

Ventouras EM, Monoyiou EA, Ktonas PY, Paparrigopoulos T, Dikeos DG, Uzunoglu NK, Soldatos CR. Sleep spindle detection using artificial neural networks trained with filtered time-domain EEG: a feasibility study. Comput Methods Programs Biomed, 2005; 78: 191-207.

Wendt SL, Christensen JA, Kempfner J, Leonthin HL, Jennum P, Sorensen HB. Validation of a novel automatic sleep spindle detector with high performance during sleep in middle aged subjects. Conference proceedings of the International Conference of the IEEE Engineering in Medicine and Biology Society; 2012: 4250-3.